J. T. K. L.
JURNAL TEKNIK KIMIA DAN LINGKUNGAN

J. Tek. Kim. Ling. 2025, 9 (2), 81-94
p-ISSN : 2579-8537, e-ISSN : 2579-9746
http://jurnal.polinema.ac.id/index.php/jtkl
DOI: http://dx.doi.org/10.33795/jtkl.v9i2.7345

Optimization of Biodiesel Production from Sunflower Oil Using Sodalite-Based Catalyst via Taguchi Method

Abdul Hamid[1,*], Amin Jakfar[1], Zeni Rahmawati[2], Muhammad Doni Armansyah[1], Tri Wahyuni[3], Tri Esti Purbaningtias[4], Ike Dayi Febriana[1], Mohammad Abdullah[5], Aurista Miftahatul Ilmah[5], Faizatur Rohmah[1]

[1]Department of Mechanical and Industrial Engineering, Politeknik Negeri Madura, Jl. Raya Camplong No. Km 4, Abacateh, Sampang 69281, Indonesia
[2]Department of Chemistry, Faculty of Science and Data Analytics, Institut Teknologi Sepuluh Nopember, Kampus ITS Sukolilo, Surabaya 60111, Indonesia
[3]Dharma Wanita 1 Senior High School, JL. Jend. A. Yani No.1 Pare, Kediri 64211, Indonesia
[4]Department of Chemistry, Faculty of Mathematics and Natural Sciences, Universitas Islam Indonesia, Jalan Kaliurang Km. 14 Sleman, Yogyakarta 55584, Indonesia
[5]Department of Maritime Technology, Politeknik Negeri Madura, Jl. Raya Camplong No. Km 4, Abacateh, Sampang 69281, Indonesia

ABSTRACT

The growing demand for alternative fuels has highlighted biodiesel as sustainable substitute for fossil diesel. In this study, biodiesel was produced from sunflower seed oil using heterogeneous catalyst synthesized from natural kaolin into sodalite via hydrothermal process. The synthesized catalyst was characterized using XRD, FTIR and SEM-EDS, confirming the transformation of kaolinite to sodalite. The transesterification reaction was conducted under varying methanol-to-oil molar ratios (1:12, 1:18, and 1:24) and temperatures (60, 65, and 70°C). A Taguchi orthogonal array (L9) was employed to statistically evaluate the effects of these parameters on methyl ester yield. Experimental results showed that both methanol ratio and reaction temperature significantly influenced biodiesel yield, with the highest yield of 90.44% obtained at 70°C and 1:18 molar ratio. Signal-to-noise ratio and ANOVA analysis indicated that the methanol-to-oil ratio was the most dominant factor (46.05%) compared to temperature (40.55%). The resulting biodiesel exhibited a flash point of 158°C, acid value of 0.06 mg-KOH/g, and iodine value of 84.06 g-I_2/100g, satisfying most ASTM D6751 and SNI 7182:2015 standards, though viscosity and density exceeded standard limits. Emission testing showed 16% reduction in CO emissions with increasing biodiesel blends, while NO and NO_x emissions slightly increased.

Keywords: biodiesel, heterogeneous catalyst, sodalite, sunflower oil, Taguchi method.

1. INTRODUCTION

The transportation system and industrial development play a crucial role in the economic growth of countries worldwide. Currently, the primary issue faced by both transportation and industrial sectors globally is energy supply, which is predominantly fulfilled by fossil fuels such as gasoline and diesel [1,2]. The rapidly increasing global energy demand, driven by population growth and economic activity, could lead to a fossil fuel crisis [3–5]. Moreover, fossil fuels emit substantial amounts of greenhouse gases [6,7]. Environmental pollution is a direct consequence of uncontrolled fossil fuel consumption and emissions from conventional energy sources [8,9]. The growing awareness of environmental impacts and stricter emission regulations have driven the search for alternative renewable fuels to replace petroleum-derived diesel [10] . In this context, biodiesel has received increasing attention as a renewable substitute for conventional diesel fuel [11]. Biodiesel has similar characteristics to petroleum diesel and can therefore be used in conventional compression ignition engines either in pure

*Corresponding author:
E-mail: ahamchimie@poltera.ac.id (Abdul Hamid)

Received : May 27, 2025
Accepted : August 11, 2025

form or blended with diesel without requiring major modifications [12,13]. Biodiesel can be produced from a wide variety of plant sources. Non-food crops such as Jatropha curcas oil [14,15], kesambi oil [16], Ceiba pentandra oil [17], and Reutealis trisperma oil [18] have been investigated as potential feedstocks. Among these, sunflower oil is currently considered a promising biodiesel feedstock due to its low free fatty acid content, high availability, and non-competition with food sources [19]. However, the efficiency of biodiesel production heavily depends on the type of catalyst used. Heterogeneous base catalysts are gaining popularity due to their reusability, high thermal stability, and reduced environmental impact compared to homogeneous catalysts. One of the most widely used materials is zeolite. Various types of zeolites have been extensively applied in previous studies for biodiesel production, such as ZSM-5 [20], Na-X zeolite [21] , zeolite-P [22], Na-Y zeolite [23], and another highly promising zeolite, sodalite [24,25].

Sodalite, a type of zeolite mineral, is among the most promising heterogeneous base catalysts due to its strong basicity, large surface area, and good chemical stability, making it a suitable candidate for transesterification reactions in biodiesel production [26]. Despite its potential, the synthesis of sodalite from natural raw materials like kaolin remains limited. Kaolin, an abundant aluminosilicate mineral, contains suitable levels of SiO_2 and Al_2O_3 for sodalite synthesis [27,28]. Through proper chemical activation and modification, kaolin can be converted into sodalite via hydrothermal treatment in an alkaline environment [29]. This process not only adds value to natural kaolin but also yields an environmentally friendly catalyst with high efficiency for biodiesel production. Utilizing kaolin as the raw material can thus make sodalite production more economical and sustainable [30].

Previous studies on biodiesel production from sunflower oil include Simbi et al. [31], who reported the synthesis of fatty acid methyl esters (FAME) from waste sunflower oil using a novel CaO/Al_2O_3 catalyst, achieving a yield of 98.23% at optimal conditions (2.5 wt% catalyst loading, 5-hour reaction time, and 60°C). Dueso et al. [12] investigated the use of antioxidant additives in sunflower biodiesel, which resulted in a 3.0% reduction in NO_x emissions and a 4.4% reduction in smoke opacity compared to pure biodiesel. CO and HC emissions increased slightly but remained lower than those of petroleum diesel. Salmasi et al. [32] produced biodiesel using a K_2CO_3 catalyst derived from talc, achieving a 98.4% yield at 338 K, with 4 wt% catalyst loading and a 6:1 methanol-to-oil molar ratio.

The methanol-to-oil molar ratio and transesterification temperature are critical factors in biodiesel production as they influence the efficiency of the transesterification reaction and the quality of the resulting biodiesel [33,34]. Methanol is the primary reactant in the formation of methyl esters (biodiesel) and glycerol by-products. An optimal methanol-to-oil ratio is crucial, as insufficient methanol leads to incomplete reactions, while excess methanol complicates product recovery and separation. Additionally, the transesterification temperature affects reaction rate and conversion efficiency, with optimal reactions typically occurring near methanol's boiling point (60–65°C) [35]. Low temperatures result in slower reactions and lower conversion, while excessively high temperatures may degrade the oil or form undesirable by-products.

Based on these issues, this study aims to optimize biodiesel production from sunflower oil using sodalite as a catalyst and the Taguchi method for process optimization. The Taguchi method offers a statistically robust approach for process optimization, requiring a relatively small number of experimental trials while still providing scientifically significant insights. In the context of biodiesel production from sunflower oil using sodalite-based catalysts, the Taguchi method is particularly effective,

as it facilitates the identification of the most influential process parameters, specifically the methanol-to-oil molar ratio and reaction temperature. The study focuses on the effects of varying methanol-to-oil ratios and transesterification temperatures on biodiesel yield, as well as emission analysis of NO, NO_x, and CO gases using the resulting biodiesel blends in a diesel engine.

2. RESEARCH METHODS

2.1 EQUIPMENT AND MATERIALS

The equipment used in the biodiesel production process includes a three-necked flask, analytical balance, hotplate magnetic stirrer, condenser tube, water pump, tubing, beaker glass, thermometer, magnetic stirrer, dropper, retort stand, separating funnel and gas analyzer. The materials required in this study include sodium aluminat purchased from Sigma Aldrich, sodium hydroxide and methanol purchased from Merck. The chemicals above use pro-analysis. Other materials used include natural kaolin from Bangka Belitung, Indonesia, demineralized water, and sunflower oil purchased from Horecaba Jaya Makmur.

2.2 SYNTHESIS OF SODALITE CATALYST

The sodalite catalyst was synthesized via a hydrothermal method using a polypropylene bottle. The molar ratio used for synthesis was $2SiO_2:Al_2O_3:3Na_2O:128H_2O$. First, 4.47 grams of sodium hydroxide (NaOH) were dissolved in 52.5 grams of demineralized water in a polypropylene bottle while stirring until fully dissolved. Then, 12 grams of kaolin were gradually added and stirred for 15 minutes until homogeneous. Subsequently, 1.8 grams of sodium aluminate ($NaAlO_2$) were added and stirred at room temperature for 24 h. The resulting mixture was aged for another 24 h at room temperature before undergoing hydrothermal treatment at 100°C for 24 h. After the hydrothermal process, the mixture was cooled, filtered to separate the solid and liquid phases, and washed with demineralized water until reaching pH of around 8–9. The solid product was then dried at 100°C in an oven for 24 h. The synthesized solid was characterized using XRD, FTIR, and SEM-EDS.

2.3 CATALYST CHARACTERIZATION

The synthesized catalyst was characterized using X-ray diffraction (XRD) with a Bruker D2 Phaser instrument and CuKα radiation (λ = 1.54 Å) within a 2θ range of 5°–60° to determine the catalyst's phase. FTIR analysis was conducted using a Nicolet Avatar 360 IR spectrometer to identify the bonds and functional groups present in the catalyst. The spectra were recorded in the 400–1400 cm^{-1} range using the KBr pellet technique. Scanning electron microscopy and energy-dispersive X-ray analysis (SEM-EDS) were performed with a Hitachi-Flexsem 1000 to observe the morphology and elemental composition of the catalyst

2.4 BIODIESEL PRODUCTION FROM SUNFLOWER OIL

The production process began with an esterification stage in which sunflower oil was reacted with methanol in the presence of sulfuric acid as a catalyst. The molar ratio of oil to methanol used was 1:12, and 2% H_2SO_4 by oil weight was added. The esterification reaction was carried out at 65°C for 2 h. After the reaction, the mixture was allowed to settle for 24 h to form two layers. The bottom layer was collected and prepared for the transesterification stage.

In the transesterification stage, the esterified oil was reacted with methanol at molar ratio of 1:12 to produce methyl esters (biodiesel). Methanol was first mixed with sodalite catalyst (2 wt% of oil) under stirring, and then added to the sunflower oil. The mixture was stirred at 900 rpm at 60°C for 2 h. After the reaction, the mixture was poured into a separating funnel to form two layers. The biodiesel layer was analyzed using GC-MS. The same steps were repeated with variations in the molar ratio of methanol to oil of 1:18 and 1:24 and transesterification temperatures of 65 and 70°C.

2.5 EXPERIMENTAL DESIGN USING TAGUCHI METHOD

This study investigated the factors affecting biodiesel production from sunflower oil, particularly the methanol-to-oil molar ratio and reaction temperature. Three levels were tested for each factor, as summarized in Table 1.

Table 1. Design factors and levels of transesterification reaction parameters.

Parameter	Level 1	Level 2	Level 3
Methanol:Oil Molar Ratio	12:1	18:1	24:1
Reaction Temperature (°C)	60	65	70

The experimental results (biodiesel yield) were analyzed using the Taguchi method and ANOVA with Minitab software. The analysis provided insights into factor contributions, signal-to-noise (S/N) ratios, and optimal parameter combinations for maximizing biodiesel production from sunflower oil.

3. RESULTS AND DISCUSSION

The X-ray diffraction analysis results for kaolin and sodalite samples are presented in Figure 1. The diffractogram shows a transformation of the characteristic peaks of kaolin into those of sodalite-type zeolite. The distinctive diffraction peaks for kaolinite are observed at 2θ values around 12.36°, a broad peak between 19.89–21.27°, 24.78°, 34.82–35.99°, 37.77–39.27°, 38.61°, and a minor peak at approximately 45.57°. These peaks are consistent with previous studies [36–38], where the characteristic kaolin peaks appear at 2θ = 12.34° and 24.64°, with broadening between 34–40°. In contrast, the sodalite sample displays new diffraction peaks at 2θ = 13.90°, 24.31°, 31.7°, 34.57°, and 42.72°, indicating the formation of the sodalite phase, as also reported by Yu et al. [39]. Moreover, the diffraction peaks of the synthesized sodalite sample exhibit a pattern consistent with the standard reference. The XRD pattern of the sodalite sample reveals the absence (disappearance) of the kaolinite phase, confirming the complete conversion to sodalite. This suggests that the kaolinite framework underwent transformation into a Si-O-Al framework during the synthesis process, which involved mixing, aging, and crystallization.

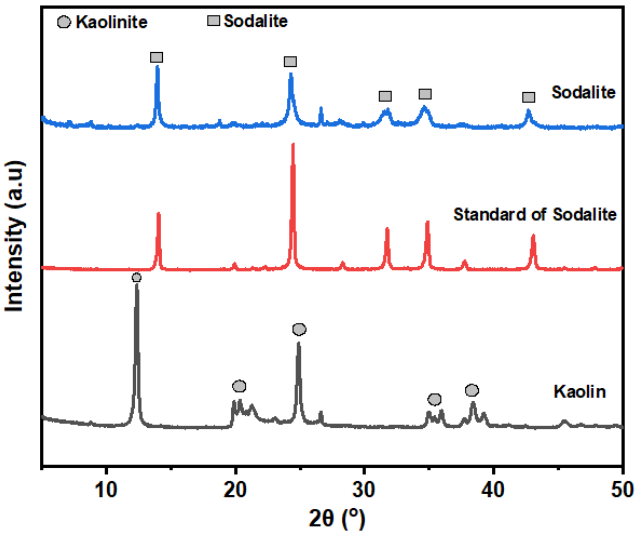

Figure 1. Diffraction of kaolin, standard and sodalite.

The FTIR spectra in Figure 2 show the differences in functional group characteristics between kaolin and sodalite. Kaolin exhibits absorption bands at 538 cm^{-1}, associated with Al–OH vibrations, and at 694 cm^{-1}, corresponding to Al-O-H bending vibrations. The bands at 753 and 792 cm^{-1} are attributed to Si–O–Al stretching vibrations [40]. The absorption in the range of 1107–1029 cm^{-1} is linked to Si–O–Si stretching vibrations [41]. These characteristic peaks of kaolin disappear in the synthesized sodalite, indicating the transformation from the kaolinite phase to the sodalite framework. The absorption bands for sodalite are observed at 988 cm^{-1} (asymmetric T-O-T stretching, where T = Si or Al), 723 cm^{-1} and 659 cm^{-1} (symmetric T-O-T stretching), and 697 cm^{-1} (Al-O-H vibration) [29]. The region between 500–650 cm^{-1} is attributed to the vibrations of four and six-membered rings in the sodalite framework [42]. The differences in absorption bands between kaolin and sodalite confirm the phase transformation, as also supported by the XRD results.

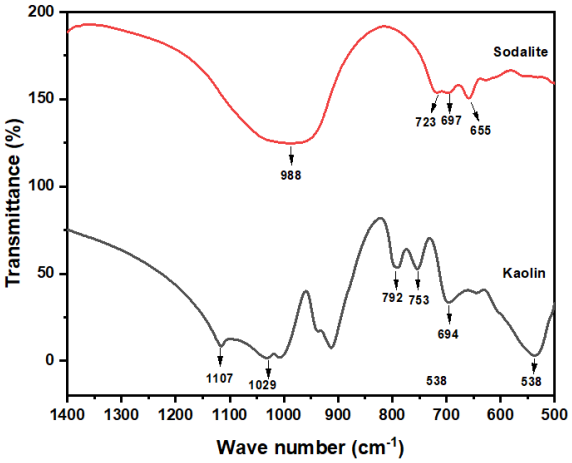

Figure 2. Diffraction of kaolin and sodalite.

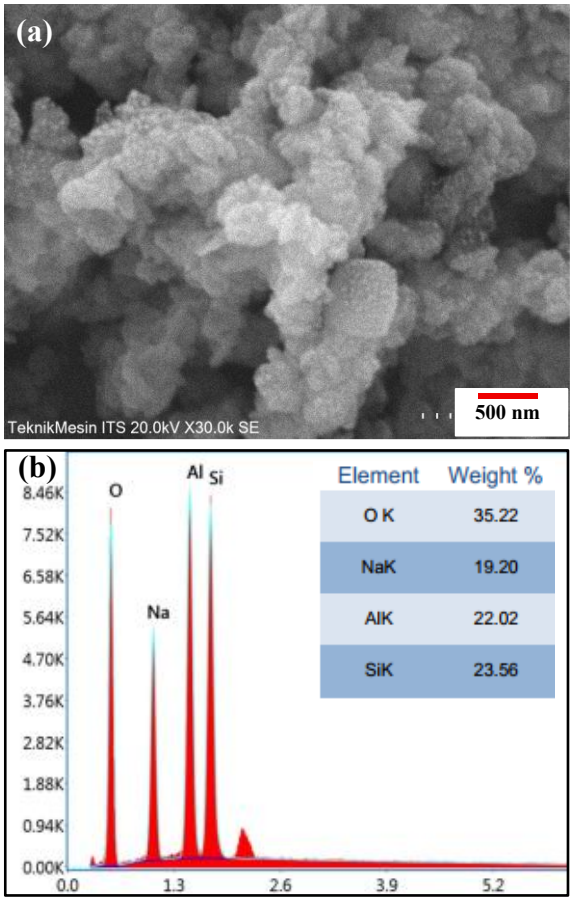

Figure 3. (a) SEM image of sodalite, (b) SEM-EDS results of sodalite.

The Figure 3 shows the surface morphology and elemental composition analysis of sodalite using a Scanning Electron Microscope (SEM) at a magnification of 30,000. The sample exhibits an irregular surface structure with a granular appearance and significant particle agglomeration. The analysis using ImageJ software revealed that the particle size distribution of sodalite was predominantly in the range of approximately 10–50 nm (Figure 4). This morphology indicates the presence of nano-sized particle aggregates forming irregular clusters. EDS analysis shows high-intensity peaks for O, Na, Al, and Si, corresponding to the main chemical composition of sodalite, with no significant contamination detected.

The presence of these elements confirms that the sample possesses a characteristic zeolitic structure, with the main constituents being oxygen, sodium, aluminum, and silicon. The highest composition was found in oxygen atoms at 35.22%, followed by silicon and aluminum at 23.56% and 22.02%, respectively.

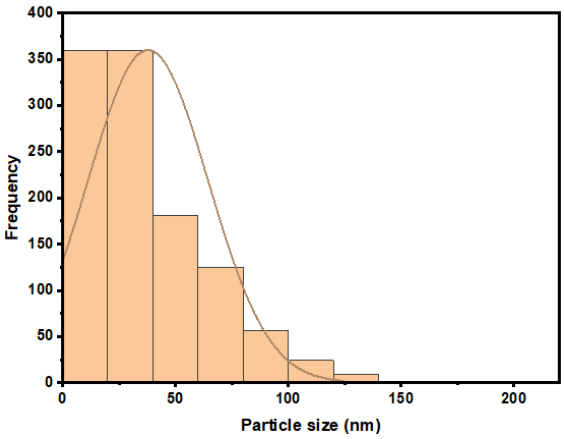

Figure 4. Sodalite particle size distribution.

Table 2. Response table for signal to noise ratios.

Level	Methanol:oil ratio	Reaction temperature (℃)
1	36.11	36.09
2	37.77	38.09
3	38.52	38.23
Delta	2.41	2.15
Rank	1	2

Table 2 presents the analysis results using the Taguchi method, which aims to identify the most optimal combination of process parameters based on the Signal-to-Noise (S/N) ratio with the "larger is better" criterion. In this context, a higher S/N value corresponds to better output quality. The table compares two process factors methanol-

to-oil ratio and reaction temperature each evaluated at three levels. The values in the columns represent the average S/N ratio for each level of the respective factors, while Δ (Delta) indicates the difference between the maximum and minimum S/N values for each factor [18]. The Rank column reflects the relative influence of each factor on the output quality. From the results, it is evident that the methanol-to-oil ratio exhibits the highest Delta value (2.41) compared to the reaction temperature (2.15), indicating that this factor has a more significant impact on the output. This is also reflected in its rank (Rank 1). This finding implies that variations in the methanol-to-oil ratio contribute more substantially to improving the quality of the output such as methyl ester conversion in biodiesel production than variations in reaction temperature. Furthermore, level 3 for both factors yields the highest S/N values, suggesting that the combination of level 3 methanol-to-oil ratio and level 3 reaction temperature represents the most optimal process parameters to achieve the best experimental results.

Table 3. Annova Analysis for S/N Ratio.

Source	DF	Seq SS	Contribution	Adj SS	Adj MS	F-Value	P-Value
Methanol:oil ratio	2	622.1	46.05%	622.1	311.07	6.88	0.051
Reaction temperature	2	547.9	40.55%	547.9	273.95	6.05	0.062
Error	4	181.0	13.40%	181.0	45.24		
Total	8	1351.0	100.00%				

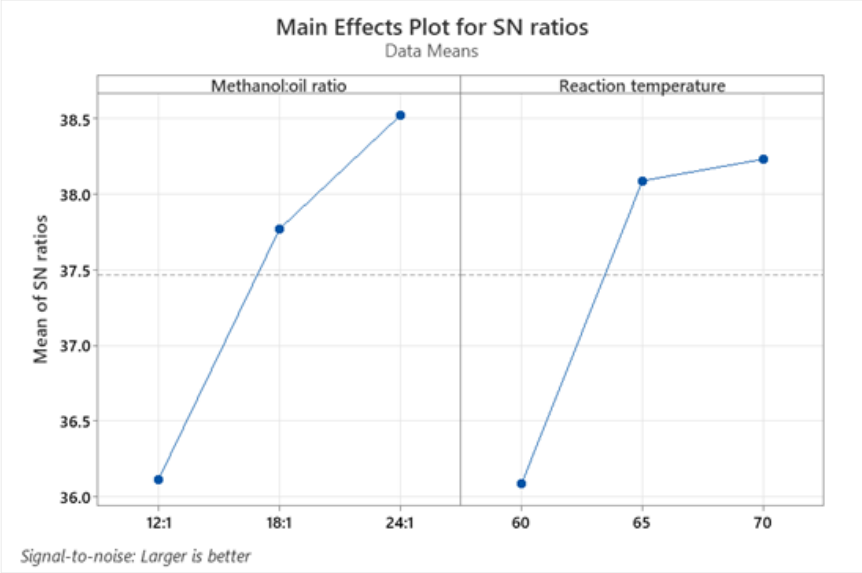

Figure 5. *S/N* plot ratio from methanol:oil ratio and reaction temperature to response of biodiesel yield.

Table 3 and Figure 5 present the results of the analysis of variance (ANOVA) conducted within the Taguchi experimental framework, aimed at assessing the significance and contribution of each factor to the total variability in the system. The two main factors analyzed were the methanol-to-oil ratio and reaction temperature, each with 2 degrees of freedom (DF), while the error term had 4 DF, resulting in a total of 8 DF. In the ANOVA, the Sequential Sum of Squares (Seq SS) and Adjusted Sum of Squares (Adj SS) quantify the variance contribution of each factor to the overall system variance

[43]. These results provide quantitative insight into the relative influence of each factor on the final outcome. The S/N ratio analysis from the response table shows that for the methanol-to-oil ratio factor, the average S/N values increase from level 1 to level 3, specifically 36.11, 37.77, and 38.52, respectively. Similarly, for the reaction temperature factor, the S/N values rise from 36.09 at level 1 to 38.23 at level 3. The Delta value (difference between maximum and minimum S/N) for the methanol-to-oil ratio is 2.41, which is higher than that of reaction temperature at 2.15, indicating that variations in the methanol-to-oil ratio have a greater impact on the output compared to temperature variations. Consequently, the methanol-to-oil ratio ranks first in terms of its influence on product quality. The ANOVA results reveal that the methanol-to-oil ratio contributes the largest proportion of variance in the system at 46.05%, followed by reaction temperature at 40.55%. The error term accounts for 13.40% of the total variance, which is within acceptable limits and indicates that most variability in the system can be explained by the factors under study.

The F-values for the methanol-to-oil ratio and reaction temperature are 6.88 and 6.05, respectively, suggesting a relatively strong influence. However, the corresponding P-values are slightly above the conventional significance threshold of 0.05, with 0.051 for the methanol-to-oil ratio and 0.062 for reaction temperature. This indicates that, while not statistically significant at the 95% confidence level, these factors remain practically important for process decision-making. Despite the P-values exceeding 0.05, the substantial contribution of both factors and their high F-values underscore the necessity of considering them in process optimization. The combination of parameter levels at their highest settings (level 3) for both factors can serve as a starting point for enhancing process efficiency.

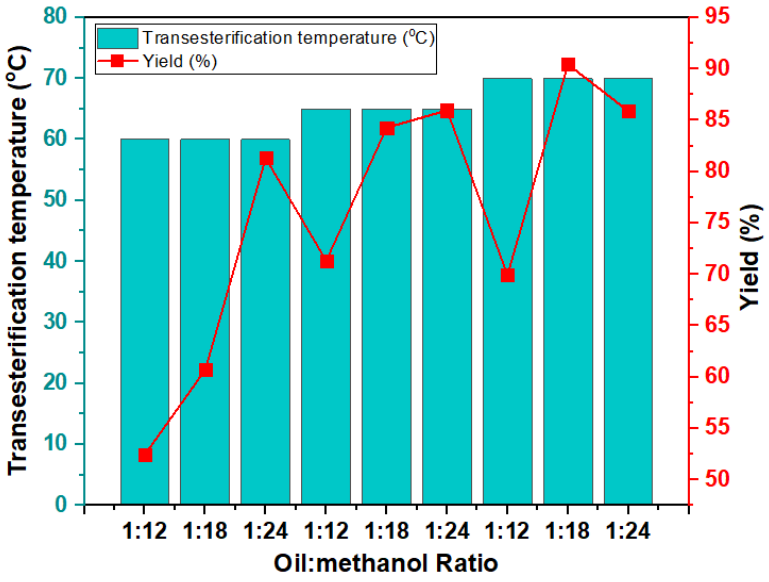

Figure 6. Biodiesel yield.

Figure 6 illustrates the relationship between the oil-to-methanol molar ratio and transesterification temperature on biodiesel yield. Generally, increasing both temperature and methanol ratio significantly improves biodiesel yield. At 60°C, yields range from 52.43% to 81.3%, indicating that this temperature is relatively suboptimal.

Raising the temperature to 65°C increases overall yield, reaching a maximum of 85.96% at a 1:24 molar ratio. Further increasing the temperature to 70°C results in

even higher yields, with the peak value of 90.44% observed at a 1:18 molar ratio. This demonstrates that the combination of elevated temperature and an appropriate methanol ratio critically influences the efficiency of the transesterification reaction [44].

From a scientific perspective, the transesterification reaction is governed by reaction kinetics and chemical equilibrium. Higher temperatures accelerate the reaction rate by increasing molecular kinetic energy; however, excessively high temperatures may cause methanol evaporation, reducing reaction efficiency or even lowering yield due to equilibrium shifts [45]. Similarly, a high methanol ratio can drive the equilibrium toward ester (biodiesel) formation, but excessive methanol may lead to emulsion formation or difficulties in product separation. The optimum yield was achieved at 70°C and a 1:18 molar ratio, which was 90.44%.

The biodiesel properties derived from sunflower oil demonstrate compliance with several standards set by ASTM D6751 and SNI 7182:2015 (Table 4). The flash point of the biodiesel was recorded at 158°C, significantly exceeding the minimum standard of 101°C, indicating good thermal stability at elevated temperatures [31]. Flash point is a critical property related to the flammability characteristics of the fuel [46].

The iodine value of 84.06 g I_2/100 g is well below the maximum allowable limit of 120 g I_2/100 g, suggesting a low degree of unsaturation and oxidation in the biodiesel [47]. Furthermore, the very low acid number of 0.06 mg KOH/g reflects a clean biodiesel quality with minimal free fatty acid content, as high acid numbers can cause severe corrosion in engine fuel systems [48].

Table 4. Properties test results of biodiesel sample.

No	Parameter	Result	Unit	Test Method	Standard (ASTM D6751)
1	Flash Point	158	^oC	ASTM D92	Min 101
2	Kinematic Viscosity at 40 °C	17.39	cst	ASTM D445	3.5-5
3	Iodine Value	84.06	g-I_2/100g	SNI 7182:2015	Max 120
4	Density at 15 °C	961	kg/m^3	Picnometer	860-900
5	Acid Number	0.06	mg-KOH/g	SNI 7182:2015	0.5
6	Pour Point	1	^oC	ASTM 2500	Max 18

However, some parameters warrant further attention. The kinematic viscosity at 40°C was measured at 17.39 cSt, exceeding the standard range of 3.5–5 cSt. This elevated viscosity may affect biodiesel performance in engines, particularly regarding fuel flow and combustion efficiency. Biodiesel viscosity values exceeding the standard can be attributed to several scientific factors, one of which is the presence of unconverted triglyceride compounds due to incomplete transesterification. Additionally, low storage temperatures may induce crystallization of certain components, thereby increasing resistance to flow. Therefore, quality control and optimization of reaction parameters are crucial to ensure that the viscosity of biodiesel complies with established standards. The density of the biodiesel was also recorded at 961 kg/m³, slightly above the recommended range of 860–900 kg/m³, which could influence the energy content per unit volume of the fuel. Nevertheless, the low pour point of 1°C indicates that the biodiesel can be used effectively in cold weather conditions while maintaining adequate fuel flow. Overall, the biodiesel exhibits promising potential, with certain properties meeting or exceeding standards, though some parameters require optimization to fully comply with operational criteria for optimal performance.

Figure 7 illustrates the relationship between fuel blend types and the concentrations of NO and NO_x gas emissions. NO_x emissions (nitrogen oxides) consist of NO (nitric oxide) and NO_2 (nitrogen dioxide), which are byproducts of the combustion process in diesel engines. The graph shows that as the percentage of biodiesel in the fuel blend increases, the NO_x emissions also tend to increase. However, a slight decrease in NO and NO_x emissions is observed when using B40 fuel. The increase in NO and NO_x emissions is relatively insignificant when transitioning from pure diesel (D100) to B30, with an approximate rise of 3 ppm for each incremental biodiesel blend.

This phenomenon suggests the existence of an optimal biodiesel blend, where the highest NO and NO_x emissions occur at B30 fuel. This is attributed to the higher oxygen content in biodiesel compared to pure diesel (D100), which generally leads to higher combustion temperatures. Elevated temperatures tend to enhance NO_x formation due to the accelerated reaction between nitrogen and oxygen in the air under high-temperature conditions. Similarly, NO emissions exhibit an increasing trend corresponding to higher biodiesel content in the fuel.

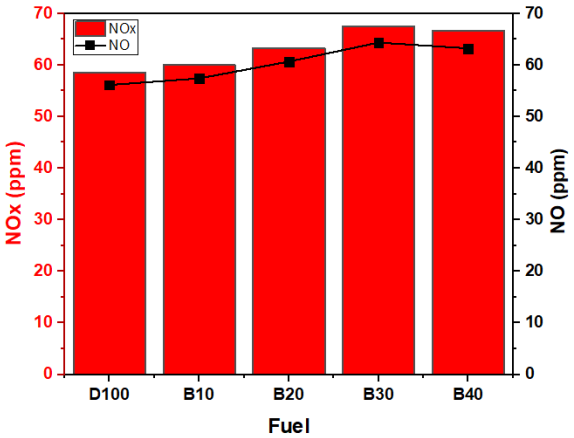

Figure 7. Results of NO and NO_x gas emission tests from fuel mixtures.

The lowest NO and NO_x emissions were recorded for D100 fuel, at 56.15 ppm and 58.5 ppm respectively, whereas the highest emissions were observed for B40 fuel, at 64.35 ppm and 67.42 ppm respectively. This corresponds to an approximate 13% increase in NO and NO_x emissions from D100 to B30. Numerous studies have reported that blending biodiesel with diesel fuel increases NO_x emissions, primarily due to the higher oxygen content in biodiesel compared to conventional diesel. These findings are consistent with previous research by Mohammad et al. [49] and Zahedi et al. [50], which also demonstrated an increasing trend in NO and NO_x emissions with higher biodiesel blend ratios.

Figure 8 illustrates the trend of decreasing carbon monoxide (CO) emissions with increasing biodiesel content in the fuel blend. Carbon monoxide is a byproduct of incomplete combustion in diesel engines. The highest CO emissions were observed with pure diesel fuel (D100), while biodiesel blends (B10, B20, B30, and B40) exhibited a gradual reduction in CO emissions. This indicates that biodiesel enhances combustion efficiency, thereby reducing CO formation. The decrease in CO emissions from biodiesel fuel is attributed to its higher oxygen content compared to conventional diesel. The oxygen present in biodiesel facilitates the oxidation of unburned carbon, converting more carbon into carbon dioxide (CO_2) rather than carbon monoxide. Consequently, higher biodiesel content in the fuel blend leads to more complete combustion, resulting in lower CO emissions.

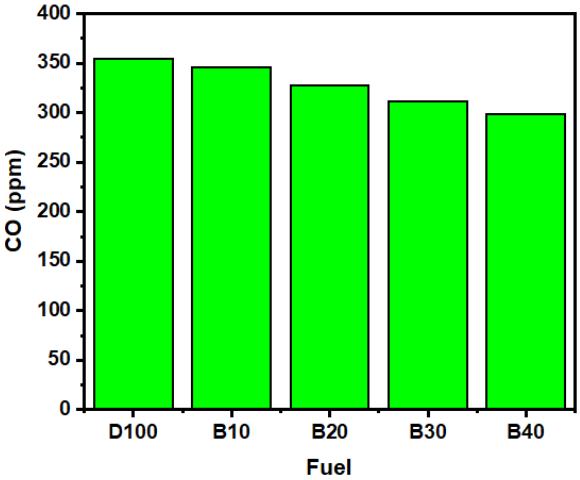

Figure 8. Results of CO gas emission tests from fuel mixtures.

The highest and lowest CO emission levels were recorded for D100 and B40 fuels, at 355 ppm and 299 ppm, respectively. This corresponds to approximately a 16% reduction in CO emissions with the B40 blend. These findings are consistent with those reported by Divyachandrika et al. [51] and Fareed et al. [52], who documented a decrease in CO emissions with increasing biodiesel blend ratios. The reduction in CO emissions highlights one of the key advantages of using biodiesel as a more environmentally friendly alternative fuel compared to pure diesel.

4. CONCLUSION

This study successfully demonstrated the potential of sodalite synthesized from natural kaolin as an effective heterogeneous catalyst for biodiesel production from sunflower oil. The optimization process using the Taguchi method revealed that the methanol-to-oil molar ratio and reaction temperature significantly influenced the biodiesel yield, with the highest yield of 90.44% obtained at 70°C and a 1:18 molar ratio. ANOVA analysis confirmed that the methanol-to-oil ratio had the most substantial contribution to yield variability (46.05%), followed by reaction temperature (40.55%). The physicochemical properties of the produced biodiesel mostly met the ASTM D6751 and SNI 7182:2015 standards, with excellent flash point and acid value, although viscosity and density slightly exceeded standard limits. Emission analysis indicated that higher biodiesel content in diesel blends reduced CO emissions by up to 16%, while NO and NO_x emissions showed a moderate increase due to improved combustion efficiency. These results highlight that sodalite-based catalysts derived from kaolin not only offer a low-cost and sustainable alternative for biodiesel synthesis but also contribute to reducing environmental pollutants.

ACKNOWLEDGMENT

The authors gratefully acknowledge Politeknik Negeri Madura for providing internal research funding under Contract No. 1139/PL34/AL.04/2024 through the PDP Scheme. The researchers also thank Institut Teknologi Sepuluh Nopember Surabaya for their collaborative support in research activities

REFERENCES

[1] D. T. Oyekunle, E. A. Gendy, M. Barasa, D. O. Oyekunle, B. Oni, S. K. Tiong, Review on Utilization of Rubber Seed Oil for Biodiesel Production: Oil Extraction, Biodiesel Conversion, Merits, and Challenges, *Clean. Eng. Technol.*, vol. 21, pp. 100773, 2024.

[2] W. N. A. W. Osman, J. K. L. Min, S. Samsuri, Exploring the Thermal Properties of Biodiesel After Purification Via Solvent-Aided Crystallization, *Results Eng.*, vol. 22, pp. 1–10, 2024.

[3] B. Azhar, S. Gunawan, M. Muharja, C. Avian, D. Satrio, H. W. Aparamarta, Optimization of Microwave-Assisted Extraction in The Purification of Triglycerides from Non-edible Crude Calophyllum inophyllum Oil as Biodiesel Feedstock Using Artificial Intelligence, *S. Afr. J. Chem. Eng.*, vol. 47, pp. 312–321, 2024.

[4] T. Touqeer, M. W. Mumtaz, H. Mukhtar, A. Irfan, S. Akram, A. Shabbir, U. Rashid, I. A. Nehdi, T. S. Y. Choong, Fe_3O_4-PDA-Lipase as Surface Functionalized Nano Biocatalyst for The Production of Biodiesel Using Waste Cooking Oil as Feedstock: Characterization and Process Optimization, *Energies*, vol. 13, no. 1, pp. 1–19, 2020.

[5] M. Aghbashlo, W. Peng, M. Tabatabaei, S. A. Kalogirou, S. Soltanian, H. Hosseinzadeh-Bandbafha, O. Mahian, S. S. Lam, Machine Learning Technology in Biodiesel Research: A Review, *Prog. Energy Combust. Sci.*, vol. 85, pp. 1–112, 2021.

[6] G. D. Okcu, Microalgae Biodiesel Production: a Solution to Increasing

Energy Demands in Turkey, *Biofuels*, vol. 13, no. 1, pp. 77–93, 2022.

[7] S. Vellaiyan, K. Aljohani, B. S. Aljohani, B. R. S. R. Reddy, Enhancing Waste-Derived Biodiesel Yield using Recyclable Zinc Sulfide Nanocatalyst: Synthesis, Characterization, and Process Optimization, *Results Eng.*, vol. 23, pp. 1–10, 2024.

[8] I. M. Maafa, A. A Sayed Alahl, M. O. Abd El-Magied, X. Cui, A. S. Dhmees, Eco-friendly Self-terminated Process for Preparation of CaO Catalyst Based on Chitosan Production Wastes for Biodiesel Production, *J. Mater. Res. Technol.*, vol. 30, pp. 1217–1227, 2024.

[9] M. A. Asokan, S. S. Prabu, B. Musthafa, B. Saravanan, S. Sujai, R. T. Pote, N. P. Chavan, D. S. Bhor, Effect of Antioxidants on CI Engine Characteristics of Safflower Biodiesel with Varying Fuel Injection Pressures, C*ase Stud. Therm. Eng.,* vol. 60, pp. 1–10, 2024.

[10] J. V. L. Ruatpuia, G. Halder, M. Vanlalchhandama, F. Lalsangpuii, R. Boddula, N. Al-Qahtani, S. Niju, T. Mathimani, S. L. Rokhum, Jatropha Curcas Oil a Potential Feedstock for Biodiesel Production: A Critical Review, *Fuel*, vol. 370, pp. 1–16, 2024.

[11] T. A. Mekuriaw, M. K. Abera, CaO - Catalyzed Trans-esterification of Brassica carinata Seed Oil for Biodiesel Production, *Heliyon*, vol. 10, no. 13, pp. 1–15, 2024.

[12] C. Dueso, M. Muñoz, F. Moreno, J. Arroyo, N. Gil-Lalaguna, A. Bautista, A. Gonzalo, J. L. Sánchez, Performance and Emissions of A Diesel Engine Using Sunflower Biodiesel with A Renewable Antioxidant Additive from Bio-oil, *Fuel*, vol. 234, pp. 276–285, 2018.

[13] F. Esmi, A. K. Dalai, Y. Hu, Comparison of Various Machine Learning Techniques for Modeling The Heterogeneous Acid-catalyzed Alcoholysis Process of Biodiesel Production from Green Seed Canola Oil, *Energy Rep.*, vol. 12, pp. 321–328, 2024.

[14] C. H. Chang, H. Y. Wei, B. Y. Chen, C. S. Tan, In situ Catalyst-free Biodiesel Production from Partially Wet Microalgae Treated with Mixed Methanol and Castor Oil Containing Pressurized CO_2, *J. Supercrit. Fluids*, vol. 157, pp. 1–8, 2019.

[15] H. Teklehaimanot, N. Gupta, R. B. Nallamothu, The Impact of Al2O3 Nano Additives on Jatropha curcas Biodiesel-diesel Blend on Combustion and Emission Behavior, *Energy Convers. Manag.: X*, vol. 25, pp. 1–9, 2025.

[16] A. K. Yadav, M. E. Khan, A. Pal, U. Ghosh, Performance and Emission Characteristics of A Stationary Diesel Engine Fuelled by Schleichera Oleosa Oil Methyl Ester (SOME) Produced Through Hydrodynamic Cavitation Process, *Egypt. J. Pet.*, vol. 27, no. 1, pp. 89–93, 2017.

[17] M. Balajii, S. Niju, Banana Peduncle – a Green and Renewable Heterogeneous Base Catalyst for Biodiesel Production from Ceiba pentandra Oil, *Renew. Energy*, vol. 146, pp. 2255–2269, 2019.

[18] Z. Rahmawati, H. Holilah, S. W. Purnami, H. Bahruji, T. P. Oetami, D. Prasetyoko, Statistical Optimisation using Taguchi Method for transesterification of Reutealis Trisperma Oil to Biodiesel on CaO-ZnO Catalysts, *Bull. Chem. React. Eng. Catal.*, vol. 16, no. 3, pp. 686–695, 2021.

[19] G. M. Mathew, D. Raina, V. Narisetty, V. Kumar, S. Saran, A. Pugazhendi, R. Sindhu, A. Pandey, P. Binod, Recent Advances in Biodiesel Production: Challenges and Solutions, *Sci. Total Environ.*, vol. 794, pp. 1–15, 2021.

[20] Ł. Szkudlarek, K. Chałupka-Śpiewak, W. Maniukiewicz, M. Nowosielska, J.

Albińska, M. I. Szynkowska-Jóźwik, P. Mierczyński, CaO Catalysts Supported on ZSM-5 Zeolite for Biodiesel Production via Transesterification of Rapeseed Oil, *Appl. Catal. O-Open*, vol. 194, pp. 1–13, 2024.

[21] S. Otieno, F. Kengara, C. Kowenje, R. Mokaya, Optimization of Biodiesel Synthesis from Jatropha Curcas Oil Using Kaolin Derived Zeolite Na-X as a Catalyst, *RSC Adv.*, vol. 12, no. 35, pp. 22792–22805, 2022.

[22] M. R. Abukhadra, S. M. Ibrahim, S. M. Yakout, M. E. El-Zaidy, A. A. Abdeltawab, Synthesis of Na+ Trapped Bentonite/Zeolite-P composite as a Novel Catalyst for Effective Production of Biodiesel From Palm Oil; Effect of Ultrasonic Irradiation and Mechanism, *Energy Convers. Manag.*, vol. 196, pp. 739–750, 2019.

[23] Z. Li, S. Ding, C. Chen, S. Qu, L. Du, J. Lu, J. Ding, Recyclable Li/NaY Zeolite as A Heterogeneous Alkaline Catalyst for Biodiesel Production: Process Optimization and Kinetics Study, *Energy Convers. Manag.*, vol. 192, pp. 335–345, 2019.

[24] J. M. Shabani, O. Babajide, O. Oyekola, L. Petrik, Synthesis of Hydroxy Sodalite from Coal Fly Ash for Biodiesel Production from Waste-Derived Maggot Oil, *Catalysts*, vol. 9, no. 12, pp. 1–15, 2019.

[25] T. Aniokete, M. Ozonoh, M. Daramola, Synthesis of Pure and High Surface Area Sodalite Catalyst from Waste Industrial Brine and Coal Fly Ash for Conversion of Waste Cooking Oil (WCO) to Biodiesel, *Int. J. Renew. Energy Res.*, vol. 9, no. 4, pp. 1924–1937, 2019.

[26] M. C. Manique, L. V. Lacerda, A. K. Alves, C. P. Bergmann, Synthesis of Hydro-Sodalite as a Heterogeneous Catalyst for Reaction Kinetics of Soybean Oil Trans-Esterification, *J. Mater. Sci. & Eng.*, vol. 7, no. 6, pp. 1–6, 2018,

[27] A. Hamid, R. E. Nugraha, H. Holilah, H. Bahruji, D. Prasetyoko, Large Intraparticle Mesoporosity of Hierarchical ZSM-5 Synthesized from Kaolin Using Silicalite Seed: Effect of Aging Time and Temperature, *J. Korean Ceram. Soc.*, vol. 60, pp. 1–13, 2022.

[28] R. E. Nugraha, D. Prasetyoko, N. Asikin-Mijan, H. Bahruji, S. Suprapto, Y. H. Taufiq-Yap, A. A. Jalil, The Effect of Structure Directing Agents on Micro/Mesopore Structures of Aluminosilicates from Indonesian Kaolin as Deoxygenation Catalysts, *Micropor. Mesopor. Mat.*, vol. 315, pp. 1–13, 2021.

[29] T. Wahyuni, D. Prasetyoko, S. Suprapto, I. Qoniah, H. Bahruji, A. A. Dawam, S. Triwahyono, A. A. Jalil, Direct Synthesis of Sodalite from Indonesian Kaolin for Adsorption of Pb^{2+} Solution, Kinetics, and Isotherm Approach, *Bull. Chem. React. Eng. Catal.*, vol. 14, no. 3, pp. 502–512, 2019.

[30] M. Ulfa, A. Masykur, A. F. Nofitasari, N. A. Sholeha, S. Suprapto, H. Bahruji, D. Prasetyoko, Controlling the Size and Porosity of Sodalite Nanoparticles from Indonesian Kaolin for Pb^{2+} Removal, *Materials*, vol. 15, no. 8, pp. 1–19, 2022.

[31] I. Simbi, U. O. Aigbe, O. Oyekola, O. A. Osibote, Optimization of Biodiesel Produced from Waste Sunflower Cooking Oil Over Bi-Functional Catalyst, *Results Eng.*, vol. 13, pp. 1–13, 2021.

[32] M. Z. Salmasi, M. Kazemeini, S. Sadjadi, Transesterification of Sunflower Oil To Biodiesel Fuel Utilizing A Novel K_2CO_3/Talc Catalyst: Process Optimizations And Kinetics Investigations, *Ind. Crops. Prod.*, vol. 156, pp. 112846, 2020.

[33] L. Macheli, M. E. Malefane, L. L. Jewell, Waste-derived Calcium Oxide

Catalysts in Biodiesel Production: Exploring Various Waste Sources, Deactivation Challenges, and Improvement Strategies, *Bioresour. Technol. Rep.*, vol. 29, pp. 1–19, 2025.

[34] J. Silvaraja, N. Y. Yahya, M. M. Zainol, Y. S. Lee, Preliminary Investigations of Sustainable Magnetic Catalyst-Based Biochar Derived Spent Coffee Ground for Biodiesel Production from Waste Cooking Oil, *Cleaner Chem. Eng.*, vol. 11, pp. 100148, 2025.

[35] C. S. Damian, D. Yuvarajan, T. Raja, G. Choubey, D. B. Munuswamy, Biodiesel Production from Shrimp Shell Lipids: Evaluating ZnO Nanoparticles as A Catalyst, *Results Eng.*, vol. 24, pp. 103453, 2024.

[36] U. M. Aliyu, S. Rathilal, S. I. Mustapha, R. Musamali, E. K. Tetteh, Hydrothermal Synthesis of Kaolin-based ZSM-5 Zeolite: Effect of Synthesis Parameters and its Application for Bioethanol Conversion, *Catal. Commun.*, vol. 182, pp. 106750, 2023.

[37] S. Otieno, F. Kengara, C. Kowenje, R. Mokaya, Optimization of Biodiesel Synthesis from Jatropha Curcas Oil using Kaolin Derived Zeolite Na-X as a Catalyst, *RSC Adv.*, vol. 12, no. 35, pp. 22792–22805, 2022.

[38] S. Otieno, C. Kowenje, F. Kengara, R. Mokaya, Effect of Kaolin Pre-Treatment Method and NaOH Levels on The Structure and Properties of Kaolin-derived Faujasite Zeolites, *Mater. Adv.*, vol. 2, no. 18, pp. 5997–6010, 2021.

[39] M. Yu, D. Luo, J. Kuang, W. Yuan, Synthesis and Luminescence Properties of Eu^{3+} Doped Sodalite Phosphors Using Kaolin, *Results Phys.*, vol. 41, pp. 105887, 2022.

[40] M. E. F. Sari, S. Suprapto, D. Prasetyoko, Direct Synthesis of Sodalite from Kaolin: The Influence of Alkalinity, *Indones. J. Chem.*, vol. 18, no. 4, pp. 607–613, 2018.

[41] W. Luo, Z. Fan, J. Wan, Q. Hu, H. Dong, X. Zhang, Z. Zhou, Study on The Reusability of Kaolin as Catalysts for Catalytic Pyrolysis of Low-density Polyethylene, *Fuel*, vol. 302, pp. 1–112, 2021.

[42] Q. Song, J. Shen, Y. Yang, J. Wang, Y. Yang, J. Sun, B. Jiang, Z. Liao, Effect of Temperature on The Synthesis of Sodalite by Crystal Transition Process, *Micropor. Mesopor. Mat.*, vol. 292, pp. 109755, 2020.

[43] C. T. Oloyede, S. O. Jekayinfa, A. O. Alade, O. Ogunkunle, O. T. Laseinde, A. O. Adebayo, A. I. Abdulkareem, G. F. Smaisim, I. M. R. Fattah, Synthesis of Biobased Composite Heterogeneous Catalyst for Biodiesel Production Using Simplex Lattice Design Mixture: Optimization Process by Taguchi Method, *Energies*, vol. 16, no. 5, pp. 1–26, 2023.

[44] M. Saad, B. Siyo, H. Alrakkad, Preparation and Characterization of Biodiesel From Waste Cooking Oils Using Heterogeneous Catalyst(Cat.TS-7) based on Natural Zeolite, *Heliyon*, vol. 9, no. 6, pp. 1–13, 2023.

[45] S. P. Sabapathy, A. M. Ammasi, E. Khalife, M. Kaveh, M. Szymanek, G. K. Reghu, P. Sabapathy, Comprehensive Assessment from Optimum Biodiesel Yield to Combustion Characteristics of Light Duty Diesel Engine Fueled With Palm Kernel Oil Biodiesel and Fuel Additives, *Materials*, vol. 14, no. 15, pp. 1–23, 2021.

[46] V. G. Nguyen, M. T. Pham, N. V. L. Le, H. C. Le, T. H. Truong, D. N. Cao, A comprehensive Review on The Use of Biodiesel for Diesel Engines, *Int. J. Renew. Energy Dev.*, vol. 12, no. 4, pp. 720–740, 2023.

[47] I. Simbi, U. O. Aigbe, O. Oyekola, O. A. Osibote, Optimization of Biodiesel Produced from Waste Sunflower Cooking Oil Over Bi-Functional

Catalyst, *Results Eng.*, vol. 13, pp. 100374, 2022.

[48] J. Yang, C. Caldwell, K. Corscadden, Q. S. He, J. Li, An Evaluation of Biodiesel Production from Camelina sativa Grown in Nova scotia, *Ind. Crops. Prod.*, vol. 81, pp. 162–168, 2016.

[49] S. I. S. Mohammad, A. Vasudevan, K. D. V. Prasad, I. R. Ali, A. Kumar, A. Kulshreshta, V. S. Mann, I. B. Sapaev, T. Kalyani, M. Sina, Evaluation of Diesel Engine Performance and Emissions Using Biodiesel from Waste Oils Synthesized with Fe_3O_4-SiO_2 Heterogeneous Nano Catalyst, *Heliyon*, vol. 11, no. 1, pp. 1–16, 2025.

[50] A. Zahedi, Z. Moradi, G. Molaeimanesh, M. J. M. Ghanaei, Experimental Development of Biodiesel Fuel Derived from Freshwater Microalgae for Improved Engine Performance and Reduced Emissions, *Energy Rep.*, vol. 12, pp. 6036–6045, 2024.

[51] D. Divyachandrika, J. Hemanandh, P. Barmavatu, B. Ganesh, Enhancing Jatropha Oil Biodiesel by Using Citrus limetta Peels as A Biocatalyst: A Sustainable Way to Reduce Emissions and Enhance The Efficiency of CI Engine, *Int. J. Thermofluid.*, vol. 24, pp. 1–11, 2024.

[52] A. F. Fareed, A. S. El-Shafay, M. A. Mujtaba, F. Riaz, M. S. Gad, Investigation of Waste Cooking and Castor Biodiesel Blends Effects on Diesel Engine Performance, Emissions, and Combustion Characteristics, *Case Stud. Therm. Eng.*, vol. 60, pp. 1–13, 2024.